

Fluorescent Signal Amplification of Carbocyanine Dyes Using Engineered Viral Nanoparticles

Carissa M. Soto,^{*,†} Amy Szuchmacher Blum,[†] Gary J. Vora,[†] Nikolai Lebedev,[†] Carolyn E. Meador,[‡] Angela P. Won,[†] Anju Chatterji,[§] John E. Johnson,[§] and Banahalli R. Ratna^{*,†}

Contribution from the Center for Bio/Molecular Science and Engineering, Naval Research Laboratory, 4555 Overlook Avenue SW, Washington, D.C. 20375, Nova Research Inc., Alexandria, Virginia, 22308, and Department of Molecular Biology, Center for Interactive Molecular Biosciences, The Scripps Research Institute, 10550 North Torrey Pines Road, La Jolla, California, 92037

Received December 30, 2005; E-mail: cmsoto@cbmse.nrl.navy.mil; brr@cbmse.nrl.navy.mil

Abstract: We report enhancement in the fluorescent signal of the carbocyanine dye Cy5 by using an engineered virus as a scaffold to attach >40 Cy5 reporter molecules at fixed locations on the viral capsid. Although cyanine dye loading is often accompanied by fluorescence quenching, our results demonstrate that organized spatial distribution of Cy5 reporter molecules on the capsid obviates this commonly encountered problem. In addition, we observe energy transfer from the virus to adducted dye molecules, resulting in a highly fluorescent viral nanoparticle. We have used this enhanced fluorescence for the detection of DNA–DNA hybridization. When compared with the most often used detection methods in a microarray-based genotyping assay for *Vibrio cholerae* O139, these viral nanoparticles markedly increased assay sensitivity, thus demonstrating their applicability for existing DNA microarray protocols.

Introduction

Fluorescent organic dyes are extremely useful as reporting tools in many active areas of research, such as immunostaining of tissues and cells,^{1,2} and as reporters in various sensor configurations.^{1,3,4} In all these techniques, the sensitivity can be dictated by the number of dyes that can be attached per antibody or other binding agent. However, in practice, the number of dye molecules that can be attached is limited by quenching of the fluorescent signal.³ For example, antibodies labeled with more than six Cy5 dye molecules are virtually nonfluorescent due to the formation of nonfluorescent dye dimers that are also efficient quenchers.¹ If dimer formation is indeed the primary source of quenching for multiple Cy5 molecules attached to IgGs, then it should be possible to load many more dye molecules onto a protein if the dye–dye distances can be controlled to suppress dimer formation. In this paper, we demonstrate the use of an icosahedral viral capsid as a scaffold to increase the number of dye molecules with controlled intermolecular distances to eliminate self-quenching of Cy5.

Cowpea mosaic virus (CPMV) is a member of the comovirus group of plant viruses. CPMV infects legumes with yields

reaching 1–2 g/kg of leaves.⁵ The structure of CPMV has been determined to 2.8 Å resolution.⁶ The virus particles are 30 nm in diameter and display icosahedral symmetry formed by 60 copies of a subunit with two different proteins.⁶ The crystal structure of the wild-type (WT) virus displays no cysteine residues accessible to the solvent on the exterior of the capsid, which makes it suitable for specific insertion of the amino acid cysteine which contains a thiol on the side chain.⁷ In the current work, we used the EF-CPMV mutant.⁸ It contains a single cysteine introduced as a GGCGG loop placed between positions 98 and 99 of the large protein, resulting in a total of 60 cysteines, represented as white circles on the capsid (Figure 1). These insertions produce thiol groups on the protein capsid that are accessible to dyes⁹ and 5 nm gold colloidal particles.^{10,11} The EF-CPMV mutant is an excellent candidate as a scaffold for this work since the distance between thiol groups is 5.3 nm for neighbors around the same five-fold axis (icosahedral five-fold symmetry axis) and 6.5 nm for the next nearest neighbor on

(5) Johnson, J.; Lin, T.; Lomonosoff, G. *Annu. Rev. Phytopathol.* **1997**, *35*, 67–86.

(6) Lin, T.; Chen, Z.; Usha, R.; Stauffacher, C. V.; Dai, J.; Schmidt, T.; Johnson, J. E. *Virology* **1999**, *265*, 20–34.

(7) Wang, Q.; Kaltgrad, E.; Lin, T.; Johnson, J. E.; Finn, M. G. *Chem. Biol.* **2002**, *9*, 805–811.

(8) Wang, Q.; Lin, T.; Johnson, J. E.; Finn, M. G. *Chem. Biol.* **2002**, *9*, 813–819.

(9) Wang, Q.; Lin, T.; Tang, L.; Johnson, J. E.; Finn, M. G. *Angew. Chem., Int. Ed.* **2002**, *41*, 459–462.

(10) Blum, A. S.; Soto, C. M.; Wilson, C. D.; Cole, J. D.; Kim, M.; Gnade, B.; Chatterji, A.; Ochoa, W. F.; Lin, T.; Johnson, J. E.; Ratna, B. R. *Nano Lett.* **2004**, *4*, 867–870.

(11) Soto, C. M.; Blum, A. S.; Wilson, C. D.; Lazorcik, J.; Kim, M.; Gnade, B.; Ratna, B. R. *Electrophoresis* **2004**, *25*, 2901–2906.

[†] Naval Research Laboratory.

[‡] Nova Research Inc.

[§] The Scripps Research Institute.

(1) Gruber, H. J.; Hahn, C. D.; Kada, G.; Riener, C. K.; Harms, G. S.; Ahrer, W.; Dax, T. G.; Knaus, H.-G. *Bioconjugate Chem.* **2000**, *11*, 696–704.

(2) Schobel, U.; Egelhaaf, H.-J.; Brecht, A.; Oelkrug, D.; Gauglitz, G. *Bioconjugate Chem.* **1999**, *10*, 1107–1114.

(3) Anderson, G. P.; Nerurkar, N. L. *J. Immunol. Methods* **2002**, *271*, 17–24.

(4) 't Hoen, P. A. C.; Kort, F. d.; Ommen, G. J. B. v.; Dunnen, J. T. d. *Nucleic Acids Res.* **2003**, *31*, e20.

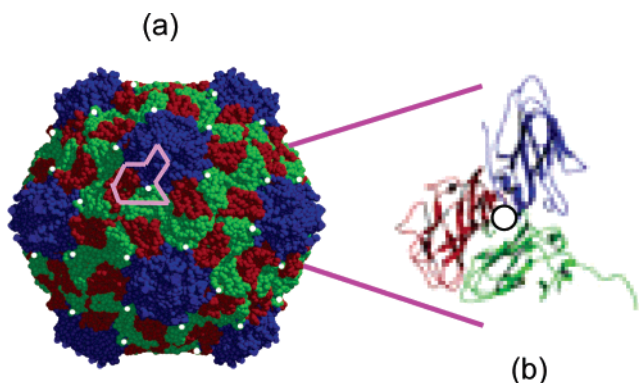


Figure 1. Cysteine mutant of CPMV. A PDB file is available for the wild-type virus (1NY7). (a) A 30 nm diameter icosahedral virus particle, EF-CPMV, made of 60 identical protein subunits containing a total of 60 cysteines (thiol-containing group shown as white circles). (b) EF-CPMV protein subunit to which a single cysteine was incorporated via the addition of a five-residue loop (GGCGG) placed between positions 98 and 99.⁸

adjacent five-fold axes.¹⁰ These distances are large enough to prevent nonfluorescent dimer formation and quenching.¹²

Experimental Section

Coupling of Maleimide–NeutrAvidin and Maleimide–Cy5 to EF-CPMV. One milliliter of a 0.07 μM solution of virus sample (EF-CPMV) in 50 mM potassium phosphate buffer pH 7.0, mixed with 51 μL of a 0.1 mM maleimide–NeutrAvidin solution (prepared according to manufacturer instructions, EZ-link maleimide activated NeutrAvidin biotin-binding protein; Amersham Biosciences Corp., Piscataway, NJ), was incubated overnight, in the dark, at room temperature (RT). Excess NeutrAvidin was removed by dialysis using a Spectrapor 100 kDa molecular weight cut-off (MWCO) dialysis membrane (Fisher Scientific, Pittsburgh, PA) against 50 mM potassium phosphate buffer pH 7.0 for 20 h, exchanging the buffer every 4 h. Most of the recovered NeutrAvidin–virus solution (88%) was mixed with 16 μL of maleimide–Cy5 solution (10 $\mu\text{g}/\mu\text{L}$ in dimethylsulfoxide (DMSO); Sigma, St. Louis, MO), corresponding to an addition of 50 molar excess of the dye with respect to the total number of thiols on the virus capsid. Reaction was carried in 20% DMSO in a final volume of 1.5 mL. The reaction was incubated overnight at RT in the dark. Excess maleimide–Cy5 was removed by using size exclusion chromatography (HiTrap desalting columns; Amersham Biosciences Corp.). Two consecutive desalting columns were run using 50 mM potassium phosphate buffer pH 7.0 as the eluent. Sample was eluted from the third column with phosphate-buffered saline (137 mM NaCl, 2.7 mM KCl, 4.3 mM Na_2HPO_4 , 1.4 mM KH_2PO_4 , pH 7.3). For preparation of a series of samples with different dye-per-virus ratios, variable amounts of Cy5 were added to the reaction mixture as described in the Supporting Information.

Biotinylated Rhodamine Assay To Determine the Presence of NeutrAvidin on NeutrAvidin-Containing Virus. A 12% portion of the remaining NeutrAvidin–virus solution was mixed with 2 μL of 1 mM biotinylated rhodamine. The reaction was allowed to proceed for 4 h, followed by dialysis to remove unbound biotinylated rhodamine. Dialysis against 50 mM potassium phosphate buffer pH 7.0 was performed using a 50 kDa MWCO dialysis membrane, over a period of 24 h, with buffer changes every 4 h.

Spectroscopic Characterization of NeutrAvidin–Cy5–Virus. UV–visible spectroscopy was performed to determine the amount of virus and dye present in the samples. The amount of virus was determined by using absorbance values of the peak at 260 nm.¹³ The amount of Cy5 dye was determined from its absorbance at 651 nm

using the extinction coefficient provided by the manufacturer (Amersham Biosciences Corp.); baselines were corrected using Peak Fit version 4.11 for samples having absorbance values <0.1 . A Varian Cary 5000 UV–vis–near-IR spectrometer (with Cary Win UV Scan Application version 3.00 software) was used for UV–visible measurements.

Fluorescence intensity for rhodamine and Cy5 was determined by their emission under excitation at 543 and 605 nm, respectively. For excitation scans of Cy5-containing samples, emission was set at 665 nm. Fluorescence measurements were performed in a FluoroLog fluorometer (Jobin Yvon Horiba, Inc., Edison, NJ; with Data Max for Windows version 2.20 software) equipped with a temperature controller which was set at 20 $^{\circ}\text{C}$.

Multiplex PCR Amplification. *Vibrio cholerae* O139 genomic DNA was obtained from the American Type Culture Collection (51394D, ATCC, Manassas, VA) and used as the template for all amplification reactions. The gene targets, probes, and primer sequences are listed in the Supporting Information. Biotinylated 45-plex polymerase chain reactions (PCRs) were performed in 50 μL volumes containing 1X PCR buffer (Qiagen Operon, Alameda, CA), 2.5 mM MgCl_2 , 200 μM dATP, dGTP, and dTTP, 20 μM dCTP, 20 μM biotin-14–dCTP (Invitrogen Life Technologies, Carlsbad, CA), 200 nM of each primer, 5 U Taq DNA polymerase (Qiagen), and 10^5 – 10^9 copies of *V. cholerae* O139 genomic DNA. Cy5–dCTP-labeled amplicons were generated in a similar manner by replacing the 20 μM biotin-14–dCTP with 20 μM Cy5–dCTP (Amersham Biosciences Corp.). The amplification reactions were performed in a Peltier thermal cycler PTC225 (MJ Research Inc., Reno, NV), with preliminary denaturation at 94 $^{\circ}\text{C}$ for 5 min, followed by 35 cycles of 94 $^{\circ}\text{C}$ for 30 s, 59 $^{\circ}\text{C}$ for 60 s, 72 $^{\circ}\text{C}$ for 90 s, and a final extension at 72 $^{\circ}\text{C}$ for 7 min. Upon completion, the amplified products were spin-purified using the UltraClean PCR cleanup kit (Mo Bio Laboratories, Carlsbad, CA) and lyophilized.

Microarray Fabrication, Hybridization, and Detection. Oligonucleotide probes were designed and synthesized with a 5'-amino modifier and 12-carbon spacer (Qiagen) and spotted onto (3-aminopropyl)triethoxysilane (silanization) + 1,4-phenylene diisothiocyanate (cross-linker)-modified glass slides for covalent probe immobilization as previously described.¹⁴ Once constructed, the spotted microarrays were blocked with a 3% bovine serum albumin–casein solution (BSA-C) for 15 min at RT, and the slides were outfitted with MAUI Mixer DC hybridization chambers (BioMicro Systems, Salt Lake City, UT). Multiplex PCR lyophilized amplicon pellets were resuspended in 20 μL of hybridization buffer (4 μL of 20X standard saline citrate (SSC), 4 μL of formamide, 1 μL of 3% BSA-C, 0.4 μL of 10% sodium dodecyl sulfate (SDS), and 10.6 μL of dH_2O), denatured for 3 min at 98 $^{\circ}\text{C}$, and immediately applied to the microarrays. Hybridizations were performed for 2 h at 63 $^{\circ}\text{C}$ on a MAUI hybridization system (BioMicro Systems). The slides were then washed twice with 4X SSC–0.2% SDS buffer for 3 min at 63 $^{\circ}\text{C}$ and twice with 2X SSC buffer for 1 min at RT. Slides that had received Cy5–dCTP-labeled amplicons were subsequently rinsed with dH_2O , dried, and scanned. Slides that were hybridized with biotinylated amplicons were fitted with 22 \times 25 LifterSlips (Erie Scientific Co., Portsmouth, NH) and prepared for probe–amplicon hybridization detection with either Cy5–streptavidin (Amersham Biosciences) or the NeutrAvidin–Cy5–EF-CPMV nanoparticle (NA–Cy5–CPMV). The microarrays were incubated with 50 μL of 10 mM Cy5–streptavidin (0.5 μL of Cy5–streptavidin, 2.5 μL of 20X SSC, 47 μL of BlockAid solution (Molecular Probes Inc., Eugene, OR)) or 1×10^{11} NA–Cy5–CPMV particles (10 μL of CPMV, 2.5 μL of 20X SSC, 37.5 μL of BlockAid solution) for 30 min at RT. Fluorescent microarray images were captured with a ScanArray Lite confocal laser scanning system (Perkin-Elmer, Torrance, CA) at laser power 80 and photomultiplier tube gain 80. Quantitative

(12) Lakowicz, J. R. In *Principles of fluorescence spectroscopy*; Plenum Press: New York, 1983; pp 257–301.

(13) Chatterji, A.; Ochoa, W. F.; Paine, M.; Ratna, B. R.; Johnson, J. E.; Lin, T. *Chem. Biol.* **2004**, *11*, 855–863.

(14) Charles, P. T.; Vora, G. J.; Andreadis, J. D.; Fortney, A. J.; Meador, C. E.; Dulcey, C. S.; Stenger, D. A. *Langmuir* **2003**, *19*, 1586–1591.

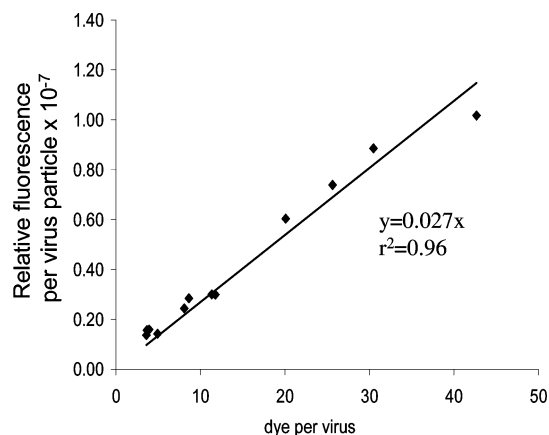


Figure 2. Concentration dependence of fluorescence intensity in NA-Cy5-CPMV. Relative fluorescence per virus particle was defined as the ratio of fluorescence at 666 nm to absorbance at 260 nm. The solid line corresponds to the linear regression from the data shown as black diamonds.

comparisons based on fluorescence intensities were made using the QuantArray analysis software package. The fluorescent signal from each microarray element was considered positive only when its quantified intensity was >2 times that of known internal negative control elements. Three independent amplification and hybridization experiments were performed from each of the DNA template dilutions (10^5 – 10^0) for the hybridization detection methods interrogated.

Results and Discussion

Fluorescence Yield as a Function of Dye per Virus.

Following standard maleimide coupling chemistry, we used the EF-CPMV as a scaffold for both Cy5 and NeutrAvidin. Thus, the NA-Cy5-CPMV can act both as a fluorescent signal-generating element (via adducted Cy5 molecules) and as a recognition element (via adducted NeutrAvidin proteins). A series of NA-Cy5-CPMV samples containing different dye-per-virus ratios (Table 1S, Supporting Information) were prepared to determine the relative fluorescence yield as a function of the number of dyes per virus. The fluorescence signal (Figure 2) increased linearly over a wide range of dye-per-virus ratios, suggesting negligible quenching in the virus conjugate even at dye loads of 42 dye/virus.

The fluorescence yield of NA-Cy5-CPMV (EF-dye, 42 dye/virus; Figure 3) was compared with two experimental controls: wild-type (WT)-dye mix (dye not bound to the WT viral protein scaffold) and free Cy5 in solution. The concentrations of both Cy5 and virus (Figure 3a) were held comparable for all samples. For all spectra, the peak at 260 nm is due to the CPMV virus, while the double peak at 605/650 nm is due to the Cy5 dye. The absorption spectra for all three samples were similar except for a 2 nm red shift in the main Cy5 absorption peak at 605/650 nm for the EF-dye sample in which the Cy5 is covalently coupled to the virus. This red shift is known to indicate coupling of Cy5 to proteins¹⁵ and confirms that, as predicted, the Cy5 molecules are covalently attached to the EF virus, but not to the wild-type virus. Figure 3b shows fluorescence intensities (relative quantum yield) under excitation at 605 nm for all three samples, normalized to the absorbance at 605 nm. Here, 605 nm is used for excitation instead of the absorbance maximum at 650 nm in these experiments so that

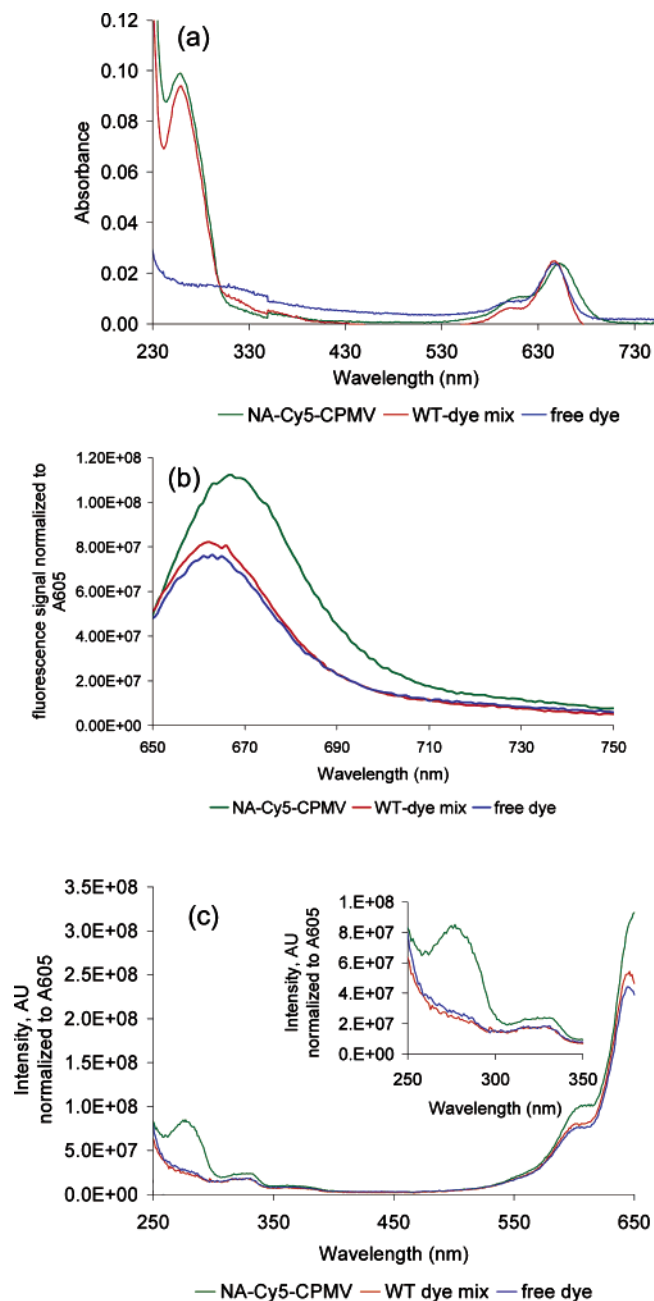


Figure 3. Spectroscopic characterization of NA-Cy5-CPMV conjugates (green), WT-dye mix (red), and free dye (blue) normalized to the absorbance at 605 nm. (a) UV-visible spectra showing absorbance of CPMV and Cy5 in the three solutions. Peaks at 260 and 651 nm correspond to virus and Cy5, respectively. The concentrations of virus were comparable for NA-Cy5-CPMV and WT-dye mix. The concentration of Cy5 is the same for all three samples. (b) Fluorescence spectra for the samples shown in (a) excited at 605 nm, normalized to the absorbance at 605 nm. Fluorescence maximum is red-shifted for NA-Cy5-CPMV, indicating that the dye is coupled to the protein. (c) Excitation scans of solutions shown in (a) and (b) with the emission set at 665 nm, normalized to absorbance at 605 nm. The peak at 280 nm on the NA-Cy5-CPMV conjugate indicates energy transfer from the virus to the dye which is not present in the negative controls of WT-dye mix and free dye. Inset shows the scan from 250 to 350 nm.

scattering at the excitation wavelength does not interfere with the emission at ~ 660 nm. Fluorescence intensities are on the same order of magnitude for all three samples; however, the covalently coupled NA-Cy5-CPMV sample shows two significant differences from the other two control samples. A red

(15) Buschmann, V.; Weston, K. D.; Sauer, M. *Bioconjugate Chem.* **2003**, *14*, 195–204.

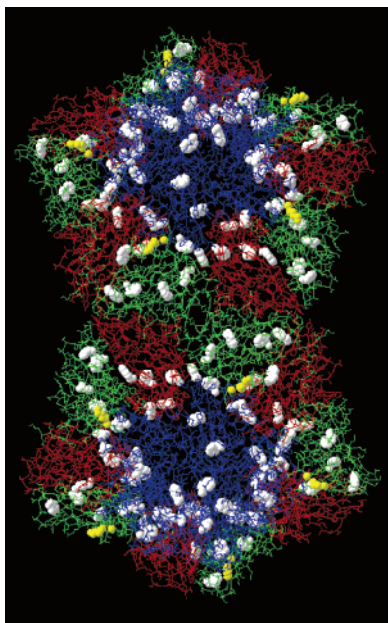


Figure 4. Tryptophan residue distribution on the EF-CPMV capsid. Crystallographic data from 10 protein subunits of EF-CPMV generated using DeepView/Swiss-Pdb Viewer version 3.7. Tryptophan residues are shown in white, and the EF loop is shown in yellow. These data were used to calculate the radial distribution of tryptophan residues with respect to the EF loop for distances from 10 to 60 Å (Table 1).

shift (2 nm) of the fluorescence maximum of the EF–dye sample in comparison to the free dye is similar to that observed in the absorption spectrum and is indicative of dye bound to protein.² Furthermore, while the normalized fluorescence intensities for the free dye and the WT–dye mix are identical within the limits of the experiment, there is a significant increase in the normalized intensity for the NA–Cy5–CPMV. This suggests that covalent coupling of the Cy5 dye to the viral scaffold enhances the fluorescence quantum yield of Cy5.

Energy Transfer between Virus and Cy5. To test the possibility of energy transfer between the protein and the dye in the NA–Cy5–CPMV samples, excitation spectra were obtained (Figure 3c) by maintaining the emission wavelength at 665 nm, corresponding to emission from the Cy5 dye, while scanning the excitation wavelength. All three samples show peaks at 605 and 650 nm, corresponding to the absorbance peaks for Cy5 (Figure 3a). However, for the NA–Cy5–CPMV sample, an additional peak at 280 nm was present. This peak, which corresponds to the absorbance of aromatic amino acid residues in CPMV, is indicative of energy transfer from the virus to the dye. Since this peak is not present in the WT–dye control, we can conclude that the dye must be coupled to the protein surface in order for energy transfer to occur. Most of the natural fluorescence of CPMV comes from the tryptophan residues,¹⁶ with an average excitation maximum at 280 nm and emission maximum at 333 nm. Cy5 absorbs between 300 and 340 nm,¹⁷ which is in the spectral range of the virus emission. A total of 840 tryptophan residues are on the virus capsid, and all are within a radius of 60 Å from the EF loop (Figure 4, Table 1) due to the symmetry of the capsid, allowing for efficient

Table 1. Tryptophan Groups in Proximity to EF Site per Protein Subunit^a

radial distance of tryptophan from the EF loop (Å) ^a	no. of tryptophans
10	0
20	7
30	13
40	21
50	37
60 ^b	55

^a From crystallographic data using DeepView/Swiss-Pdb Viewer version 3.7. A total of 840 tryptophan residues (with average excitation maximum at 280 nm and emission maximum at 333 nm) are on the virus capsid. ^b Typical Förster distances, R_0 , are between 20 and 60 Å.²

energy transfer from a large number of tryptophan residues to the EF-bound dye molecules.

Although energy transfer confirms the coupling of Cy5 dye to the CPMV scaffold, this process alone cannot explain the observed increase in fluorescence intensity. CPMV has no significant absorbance at 605 nm (Figure S1, Supporting Information), the wavelength at which signal enhancement was observed. Free Cy5 does have significant absorbance at 605 nm, suggesting that an increase in the quantum yield for emission in the Cy5 molecules due to attachment to the CPMV scaffold, rather than a direct contribution of the viral scaffold, is responsible for the observed enhancement. An enhancement in fluorescence intensity upon binding, ascribed to environmental effects on the dye, was previously observed for Cy3, but not for Cy5.¹ Research is currently underway to better understand how the CPMV microenvironment increases the overall fluorescence yield for the Cy5–CPMV complex (see Figures 2S and 3S, Supporting Information).

Enhancing Sensitivity in a DNA Sensor Platform. As the use of DNA microarray technology enables the rapid and simultaneous interrogation of thousands of genetic elements, it has quickly become a preferred tool for applications in DNA and RNA sequence analysis, gene expression profiling, genotyping of single-nucleotide polymorphisms, and the molecular detection of pathogenic organisms.^{18,19} However, despite its tremendous utility, one of the major recurrent problems in the use of DNA microarray technology has been assay sensitivity and the need for target or signal amplification. Assay sensitivity, especially in the context of pathogen detection, is one of the most important factors to consider when developing microarray-based tools and protocols. As a result, most attempts to improve DNA microarray detection sensitivity are approached by employing nucleic acid amplification strategies to amplify the amount of specific target present prior to microarray hybridization (target amplification).^{20–22} As a more recent complementary strategy, attempts to increase the signal generated by each label or hybridized DNA molecule (signal amplification) also have been developed.^{23,24}

(16) Da Poian, A. T.; Oliveira, A. C.; Silva, J. L. *Biochemistry* **1995**, *34*, 2672–2677.

(17) Heilemann, M.; Margeat, E.; Kasper, R.; Sauer, M.; Tinnefeld, P. *J. Am. Chem. Soc.* **2005**, *127*, 3801–3806.

(18) Wang, D.; Coscoy, L.; Zylberberg, M.; Avila, P. C.; Boushey, H. A.; Ganem, D.; DeRisi, J. L. *Proc. Natl. Acad. Sci. U.S.A.* **2002**, *99*, 15687–15692.

(19) Duggan, D. J.; Bittner, M.; Chen, Y.; Meltzer, P.; Trent, J. M. *Nat. Genet.* **1999**, *21*, 10–14.

(20) Vora, G. J.; Meador, C. E.; Stenger, D. A.; Andreadis, J. A. *Appl. Environ. Microbiol.* **2004**, *70*, 3047–3054.

(21) Andras, S. C.; Power, J. B.; Cocking, E. C.; Davey, M. R. *Mol. Biotechnol.* **2001**, *19*, 29–44.

(22) Lisby, G. *Mol. Biotechnol.* **1999**, *12*, 75–99.

(23) Lee, T. M. H.; Li, L. L.; Hsing, I. M. *Langmuir* **2003**, *19*, 4338–4343.

(24) Greninger, D. A.; Pathak, S.; Talin, A. A.; Dentinger, P. M. *J. Nanosci. Nanotechnol.* **2005**, *5*, 409–415.

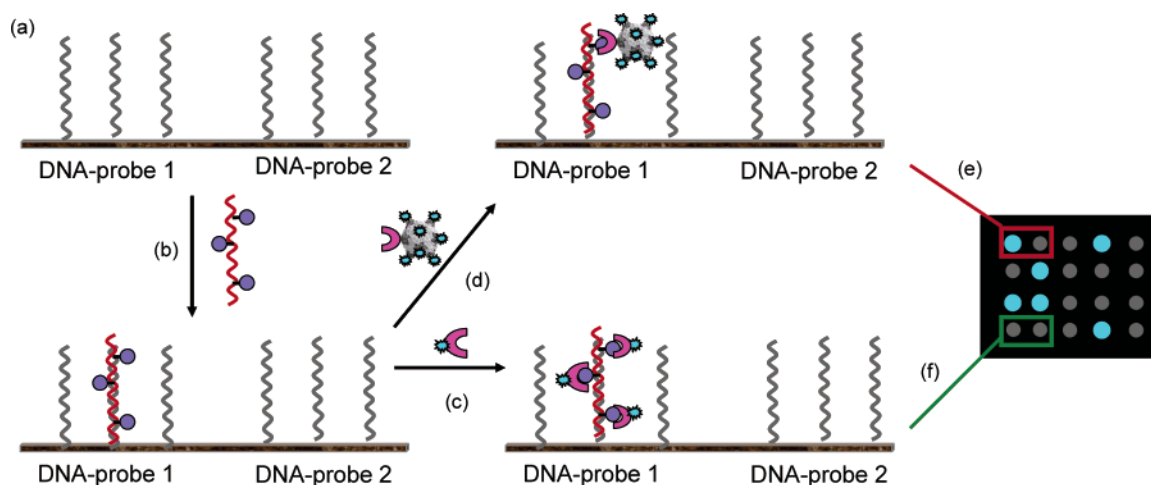


Figure 5. DNA microarray detection scheme. (a) DNA oligonucleotides 1 and 2 (probes) are immobilized in a microarray format on glass slides. (b) DNA probe 1 hybridizes with a previously amplified and biotinylated target DNA molecule. This hybridization event is detected using (c) streptavidin–Cy5 or (d) NA–Cy5–CPMV. (e) Quantification post-detection indicates a true positive signal for the NA–Cy5–CPMV detection method (blue spot, hybridization with DNA probe 1) or a true negative signal (gray spot, nonhybridization with DNA probe 2). (f) A false negative signal (gray spot) is observed for streptavidin–Cy5 as the total number of fluorophores at the DNA probe 1 spot results in the generation of a signal that is below the detection threshold (or background).

As DNA microarrays consist of an array of spatially immobilized cDNA or DNA oligonucleotide elements (probes), the signal intensity and detection sensitivity for each arrayed element are determined by the amount of label that can be localized at the hybridization reaction site. Thus, an obvious and practical signal amplification strategy to improve detection sensitivity would be to increase the amount of fluorophores per reaction site post-hybridization. However, one limitation of such a strategy is the possible self-quenching of fluorophores when they are not adequately separated from each other. Here, we use CPMV–dye complexes as a highly fluorescent recognition element for current DNA microarray applications to provide a proof-of-principle demonstration of sensitivity enhancement in a sensor platform.

DNA Detection Overview. The NA–Cy5–CPMV acts as both a fluorescent signal-generating element (via adducted Cy5 molecules) and a recognition element for DNA molecules containing biotin (via adducted NeutrAvidin proteins). Figure 5 shows the pathogen detection procedure schematically, demonstrating how NA–Cy5–CPMV can enhance sensitivity by increasing the number of dyes per biotin binding event, thus increasing the local concentration of dye vs standard techniques.

Detection and Genotyping of *V. cholerae* 0139. Having demonstrated successful dye adduction and the absence of fluorophore quenching, we sought to test the utility of the NA–Cy5–CPMV nanoparticles in a comparative study for the detection and genotyping of *V. cholerae* 0139 with the two most commonly used methods for microarray hybridization detection. Three detection methods were compared: (i) direct enzymatic incorporation of Cy5–dCTP during DNA amplification (Figure 6a), (ii) direct enzymatic incorporation of biotin–14–dCTP during DNA amplification followed by detection with Cy5–streptavidin (Cy5–streptavidin, Figure 6b), and (iii) direct enzymatic incorporation of biotin–14–dCTP during DNA amplification followed by detection with NA–Cy5–CPMV (Figure 6c). As expected, when the amount of template DNA was not limiting (i.e., 10^5 genomic copies, Figure 6d), each of the three methods tested reliably detected 100% of the targeted genes. However, as the amount of template DNA was decreased

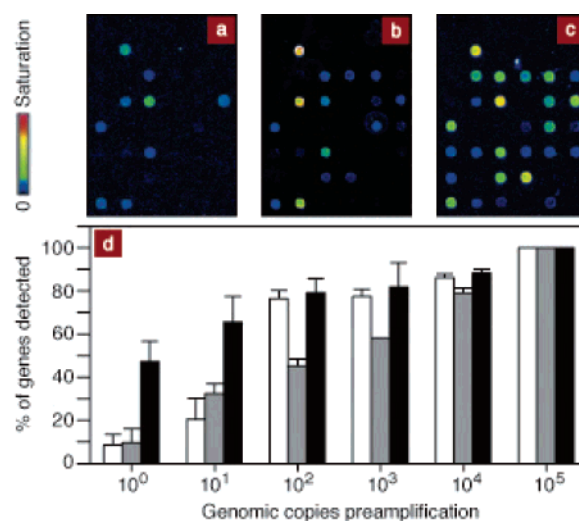


Figure 6. Comparison of NA–Cy5–CPMV with commonly utilized microarray hybridization detection methods. Fluorescent microarray hybridization profiles of *V. cholerae* 0139 amplified DNA (10^1 genomic copies starting material) detected via (a) direct incorporation of Cy5–dCTP, (b) Cy5–streptavidin, and (c) NA–Cy5–CPMV, 42 dye/virus. (d) Graphical representation of the percentage of targeted genes detected as a function of preamplification genomic DNA copy number: Cy5–dCTP (white), Cy5–streptavidin (gray), and NA–Cy5–CPMV (black). The data shown represent means \pm standard deviation (SD) of three independent amplification and hybridization experiments.

via serial dilution, the viral nanoparticles outperformed the other two detection methods with respect to the percentage of targeted genes detected (Figure 6d). This is clearly highlighted at the lowest template concentrations of 10^0 and 10^1 (Figure 6a–d). Thus, in direct comparison with the two most often used methods of microarray hybridization detection, the NA–Cy5–CPMV nanoparticles provided the greatest overall detection sensitivity. It is important to note that, while a case could be made for polymerase-mediated label incorporation bias (Cy5–dCTP versus biotin–14–dCTP) when comparing the detection sensitivities of the Cy5–dCTP direct incorporation method with the NA–Cy5–CPMV, that case cannot be made when comparing Cy5–streptavidin and NA–Cy5–CPMV, as the biotin–14–

dCTP labeling method was used for both. Thus, the increase in detection sensitivity can be attributed solely to the fluorophore loading and the absence of fluorophore quenching. The results suggest that these nanoparticles have immediate utility for the detection of trace amounts of pathogen nucleic acids, as the enhancement in detection sensitivity improves the lower limits of detection (genomic copy number or organisms) and reduces the risk of false negative determinations at low pathogen concentrations.

Conclusions

This study demonstrates the incorporation of >40 dye molecules on a 30 nm viral nanoparticle. By choosing appropriate reactive groups to covalently couple the dyes, it is possible to control dye–dye distances on the engineered virus, thus preventing nonfluorescent dimer formation and subsequent quenching, two major limitations when overloading other carrier proteins, such as IgG. In addition to the lack of quenching in NA–Cy5–CPMV, we also observed an enhancement of fluorescence output in comparison to similar molar amounts of dye in solution. Although some additional fluorescence enhancement is attributed to energy transfer from the tryptophan groups on the surface of the virus to nearby Cy5 molecules, energy transfer alone does not explain the observed increase in quantum yield for Cy5 molecules coupled to CPMV. Further research is underway to understand the fluorescence of the dye–virus combined system.

Beyond allowing for the controlled distribution of dye molecules, the virus also offers the additional advantage that a variety of reactive groups are available to couple other proteins, which may serve as a recognition element for detection of

pathogenic DNA and toxins,²⁵ making it versatile for several applications. This strategy may be transferable to other viral particles or protein scaffolds that may offer similar control of reactive group positioning. Finally, although we have specifically addressed the use of NA–Cy5–CPMV for microarray-based pathogen detection and genotyping assays, this tool may also have utility in any number of other microarray formats for the detection of single-nucleotide polymorphisms, host expression profiling, and simultaneous two-color or comparative expression profiling analyses. The enhancement in sensitivity afforded by the viral nanoparticles provides the opportunity to confidently detect small but significant changes in gene expression. The engineered EF-CPMV mutant can be readily manipulated. This fact, combined with chemical cross-linking flexibility, permits a plethora of molecular recognition, dye-loading, and multiplexing possibilities to develop viral nanoparticles that enhance assay sensitivity.

Acknowledgment. The authors thank Ellen R. Goldman and James G. Kushmerick for their comments on the manuscript. This work was supported by the Office of Naval Research.

Supporting Information Available: UV–visible spectrum of EF virus, additional fluorescence and excitation spectra, a table describing detailed preparation of NeutrAvidin–dye–virus series, and a table of gene targets, probes, and primer sequences. This material is available free of charge via the Internet at <http://pubs.acs.org>.

JA058574X

(25) Sapsford, K. E.; Soto, C. M.; Blum, A. S.; Chatterji, A.; Lin, T.; Johnson, J. E.; Ligler, F. S.; Ratna, B. R. *Biosens. Bioelectron.* **2006**, *21*, 1668–1673.